*Bangladesh Journal of Physics, Vol. **31**, Issue 2, pp. 83 – 105, December 2024*

ROLE OF LOCAL FIELDS IN INTERIONIC INTERACTIONS ON ATOMIC TRANSPORT PROPERTIES OF LIQUIDS Ti, Mn, AND Pt

MD. SHAKIL KHAN[1] AND R. C. GOSH[2,*]

[1]*Department of Theoretical Physics, University of Dhaka, Dhaka-1000, Bangladesh*
[2]*Department of Physics, University of Dhaka, Dhaka-1000, Bangladesh*

**Corresponding author e-mail: ratan@du.ac.bd*
Received on 01.07.2024, Revised received on 22.10.2024, Accepted for publication on 22.10.2024

DOI: *https://doi.org/10.3329/bjphy.v31i2.79522*

ABSTRACT

Temperature-dependent atomic transport properties, namely diffusion coefficient (D) and shear viscosity coefficient (η) of liquids Ti, Mn, and Pt, have been studied utilizing the Brettonet-Silbert (BS) pseudopotential with five different local field correction functions (LFCFs). The liquid structure is determined by both Variational modified Hypernetted Chain (VMHNC) integral equation theory and the Linearized Week-Chandler-Andersen (LWCA) perturbation method, which provides an acceptable pair correlation function, $g(r)$, through the above-mentioned potential of the concerned LFCFs. Then $g(r)$ is linked to the universal scaling laws (USLs) of Rosenfeld, Dzugutov, and Li to determine D and η. The results show that D increases, and η decreases with increasing temperature, as expected. D obtained using the LFCF of Sarker et. al. (S) provides excellent results for liquids Mn and Pt, while that of Taylor et al. (T) works well for liquid Ti. In the case of η, the LFCF of Sarker et. al. (S) works reasonably well compared to the available theoretical value and experimental data than any other LFCFs for all concerned systems.

Keywords: *Liquid metals, Transport coefficients, Pair correlation function, Local Field Correction Function*

1. INTRODUCTION

Transition metals are generally good conductors of heat and electricity and tend to crystallize in body-centered cubic (BCC), cubic close-packed (CCP), or hexagonally close-packed (HCP) structures. These characteristics have made them appealing to the researcher. From a long time ago to the current decade, atomic transport coefficients, for example, diffusion coefficient (D) and shear viscosity coefficient (η) of liquid metals, have drawn the focus of scientists by virtue of their wide range of useful applications in engineering, which includes binary solidification, glass formation, rate control of chemical reactions, and basic research in academia and industry [1-4]. Liquid and solid phases of a material can be distinguished by its dynamical diffusion properties. In a liquid, atoms may diffuse themselves without the need for defects like vacancies and interstitials, which sets them apart from a solid's process [5]. Furthermore, the self-diffusion coefficient is frequently calculated indirectly that is, with a low degree of accuracy from a measured quantity, such as a concentration profile. Furthermore, there are not many systems that have been studied experimentally [6]. Apart from that, the findings of liquid metal transport coefficients have been applied in the research fields of chemistry, metallurgy, industry, and biophysics [7].

D and η of liquid metals are very sensitive to externally generated disturbances like convection effects, so measuring it experimentally is a challenging issue. However, both theoretical and computer simulation techniques have been successful in studying these above-mentioned properties. It has been observed from the available literature [8] that the best estimate of the above-mentioned properties of liquid alkali metals depends on the effective pair interaction determined from the model pseudopotential. The *d* bands of transition metals are incomplete. It is often known that transition metal is challenging to deal with conceptually when it has a strong *d* property. However, the *d* bands have a major impact on their physical characteristics through *s*-*d* mixing, also known as *s*-*d* hybridization. Therefore, a complete description of these systems requires a model that can take into account both *sp* and *d* band effects in the interionic interactions [9-11]. Inter-ionic interactions can be obtained from Harrison's model [12], Wills and Harrison's model [13], Ashcroft's model [14], Oli's model [15], Bretonnet and Silbert (BS) pseudopotential model [16], empty core (EMC) model [17], pair-wise potentials for condensed matter containing atoms with closed shells, as introduced by Jones in 1924 and Morse in 1929 [18], many-body EAM potential [19, 20], bond order potentials have been developed for covalent solids by Tersoff in 1988 [21]. Amongst these, the BS pseudopotential model has demonstrated efficacy in the computation of thermodynamics [9], electron transport [22, 23], atomic transport [24], and liquid metal surface properties [8, 25]. The interaction between electrons and ions is the main focus of the pseudopotential model, which eventually leads to the potential of interionic pair through second-order perturbation theory. The advantage of the above-described BS theory is its ability to take into account contributions from the *s*-*p* and *d* bands for transition metals.

Furthermore, recent research by Gosh et al. [26] illustrates that changes in the profile of the BS model potential, due to changes in model parameters and LFCFs, can affect the transport properties of liquid Al. Recently, the impacts of various local field corrections have been examined for electrical transport coefficients of liquid alloys in an investigation of Aditya M. Vora [27] which likewise incorporates local field corrections in model potential. In the meantime, Md Salah Uddin studied surface (surface tension, γ) and atomic transport (*D* and η) of liquid simple metals where they observed the effect of LFCFs in the pseudopotential model [8]. In the mentioned research, the local field correction function in the pseudopotential model makes a major difference and has a considerable impact on the outcomes. That is why in this study, five different LFCFs namely Vashishta-Singwi (VS) [28], Taylor (T) [29], Ichimaru-Utsumi (IU) [30], Farid et al. (F) [31], and Sarkar et al. (S) [32] are integrated to screen BS model potential.

However, to determine atomic transport properties in relation with structural properties or $g(r)$ is mandatory. As a result, multiple efforts have been made to comprehend the atomic motion of liquids using various theoretical frameworks and computer simulation techniques. Among these, theoretical methods including linear trajectory theory, small-step diffusion theory, hard-sphere (HS) theories, and universal scaling schemes are frequently employed [1, 33-38]. Technologists and metallurgists have been tempted to scaling methods [35-40] to determine transport coefficients theoretically, particularly for melts at high temperatures [24]. Following Dzugutov [35], Li et al. and Rosenfeld et. al. has very recently come up with new USLs between the excess entropy (S_{ex}) and the viscosity coefficient [37, 38]. Also, in ref. [41] *D* and η of liquid transition metals including Ti and Mn have been successfully calculated

using the USL proposed by Dzugutov and Li et. al with $g(r)$ of HS theory of Percus-Yevick (PY) [42]. In this study, to obtain the pair distribution function $g(r)$, which is necessary to calculate S_{ex}, both the VMHNC [43] and LWCA [44] methods have been employed as they have already been proven to be successful in various studies of liquid transition metals [45, 46].

As far as we are aware, no study has been reported on temperature-dependent D and η of liquids Ti, Mn, and Pt using USLs of Dzugutov, Li, and Rosenfeld incorporating BS pseudopotential with various local field corrections along with VMHNC theory and LWCA perturbation theory, simultaneously. This study will therefore be an intensive test to see which LFCF of the pseudopotential model, in combination with both VMHNC and LWCA theory, are capable of providing better results of D and η for our concerned systems that are consistent with existing experimental and theoretical evidence.

2. THEORY

2.1. VMHNC integral equation theory

Static structure factor and its Fourier transform known as $g(r)$, is a crucial component in the study of liquid metals. It will enable us to study the both structural and atomic transport properties of liquid metals. Using a closure relation, VMHNC theory ultimately provides $g(r)$ by solving the well-known Ornstein-Zernike (OZ) [47] equation for the direct correlation function ($c(r)$) for an isotropic and homogeneous liquid system. Rosenfeld and Ashcroft came up with this hypothesis. That equation can be represented as,

$$h(r) = c(r) + n\int dr'\, h(|r - r'|)c(r') \tag{1}$$

where $h(r) = g(r) - 1$ is the total correlation function and n represents the number density.
The closure relation is attached to this equation as,

$$c(r) = h(r) - \ln g(r) \exp[\beta V(r) + B(r)] \tag{2}$$

$$g(r) = \exp[h(r) - c(r) - \beta V(r) - B(r)]. \tag{3}$$

Where $V(r)$ denotes the effective pair potential, $B(r)$ is the bridge function and β is defined as one over temperature times Boltzmann constant k which is $1/kT$. If we use this bridge function, $B(r) = B_{PY}^{HS}(r, \zeta)$ then we will get Modified hypernetted chain (MHNC) free energy in terms of β, n, and ζ. If ζ is a function of β and n which is $\zeta = \zeta(\beta, n)$ then the VMHNC condition becomes,

$$\frac{df^{VMHNC}(\beta,n,\zeta)}{d\zeta} = 0 \tag{4}$$

where $$f^{VMHNC}(\beta, n, \zeta) = f^{MHNC}(\beta, n, \zeta) - f_{PY}^{MHNC}(\zeta) + f^{CS}(\zeta). \tag{5}$$

Here, f^{MHNC} is the reduced Helmholtz free energy of the MHNC integral equation theory in the case of using the HS distribution of PY and bridge functions in association with packing fraction, ζ. f^{CS} is the Helmholtz free energy while using the Carnahan-Starling (CS) approximation. ζ is calculated by minimizing the Helmholtz free energy.

2.2. LWCA perturbation theory

The Week-Chandler-Andersen (WCA) theory [48] serves as the foundation for the LWCA theory of Meyer et al. WCA theory defines the blip function as:

$$b(r) = y_\sigma[\exp(-\beta V(r)) - \exp(\beta V_\sigma(r))] \tag{6}$$

where the quantities $V(r)$ and $V_\sigma(r)$ stand for the attractive and repulsive parts of the potential, respectively and y_σ is the cavity function connected to the HS distribution function and is continuous at $r = \sigma$. For $r > \sigma$, it is identical to the HS distribution function, $g(r)$.
Plotting the function $r^2 b(r)$ results in the appearance of a feature that resembles two sharp teeth. Right-angle triangles have been used in the LWCA theory to approximate this. Following that, Bessel's functions are used to expand the Fourier transformation of $b(r)$. The teeth in the LWCA are typically represented by right triangles. In that case, $b(r)$'s Fourier transform yields,

$$b(q) = 4\pi \int_0^\infty b(r) r^2 \frac{\sin(qr)}{qr} dr \tag{7}$$

2.3. BS pseudopotential model

Brettonet and Silbert developed a model potential for interionic interaction in liquid transition metals. This potential stems from Oli's model [15]. Brettonet and Silbert employed the distorted plane wave approach, initially introduced by Swan [49] and afterward strengthened by Oli, where in 3 dimensions, the phase shift determines the potential. It is based on the hybridization of the *s*-*p* and *d*-bands called *sd* mixing. Thus, the electron-ion interaction that yields effective *sd* hybridization in a metallic system can be expressed as follows

$$W(r) = \begin{cases} \sum_{l=1}^{2} B_l \exp\left(-\frac{r}{la}\right) & \text{for } r < R_c \\ -\frac{Z_s e^2}{r} & \text{for } r > R_c \end{cases} \tag{8}$$

where a, R_c, and Z_s represent the softness parameter, core radius, and effective *s*-electron occupancy number, respectively. Within the core radius R_c, the form of the assigned potential may be expressed by a Dirichlet series. The first two terms of this series are adequate to achieve satisfactory convergence. The term outside the core refers to the electron-ion Coulomb interaction in its most elementary manifestation. In the BS potential model, the coefficients within the core are represented in terms of three parameters indicated above and obtained by imposing the continuity approximation of $W(r)$ and its first derivative at $r = R_c$. These coefficients and also the unscreened form factor, $W_0(q)$ are provided in ref. [16].
Finally, the effective interionic pseudopotential is given by (in a.u.)

$$V(r) = \frac{Z_s^2}{r}\left(1 - \frac{2}{\pi}\int F_N(q) \sin(qr)\, dq\right) \tag{9}$$

where $F_N(q)$ denotes the normalized energy wavenumber characteristic and is expressed as

$$F_N(q) = \left(\frac{q^2}{4\pi n Z_s e^2}\right)^2 W_0^2(q)\left[1 - \frac{1}{\epsilon(q)}\right][1 - G(q)]^{-1} \tag{10}$$

where, $\epsilon(q)$ and $G(q)$ correspond to the dielectric function and LFCF in the momentum space, respectively. Relation between them is

$$\epsilon(q) = 1 - \left(\frac{4\pi e^2}{q^2}\right)\chi(q)[1 - G(q)] \tag{11}$$

Here, $\chi(q)$ represents the Lindhard function. To examine the impacts of exchange and correlation effects, the current analysis incorporates LFCFs namely VS [28], T [29], IU [30], F [31], and S [32]. These are the specifics of each local field adjustment. A formulation for local-field correction has been developed by VS and is provided by:

$$G(q) = A_{VS}(1 - e^{-B_{VS}(\frac{q}{k_F})^2}) \tag{12}$$

Given values of self-consistent $G(q)$ values for $r_s = 1 - 6, 10$ are used to calculate A_{VS} and B_{VS}, which are constants. These numbers are provided in ref. [28], and they are only applicable when $q \leq 2q_f$.

The analytical formula for the LFCF proposed by Taylor (T) fully meets the compressibility sum rule and is used to represent the function. It encompasses the general characteristics of the many LFCFs proposed before 1972 and is the most often used one. Here's what he formulated:

$$G(q) = \frac{q^2}{4k_F^2}[1 + \frac{0.1534}{\pi k_F^2}] \tag{13}$$

By using Monte-Carlo and variational approaches, it has been confirmed that the hypothesis offered by IU, is accurate and internally consistent. The formulation of the dielectric screening function by IU is as follows:

$$G(q) = A_{IU}Q^4 + B_{IU}Q^2 + C_{IU} + [A_{IU}Q^4 + \left(B_{IU} + \frac{8}{3}A_{IU}\right)Q^2 - C_{IU}]\frac{4-Q^2}{4Q}\ln\left|\frac{2+Q}{2-Q}\right| \tag{14}$$

A LFCF of the following form has been provided by Farid et. al. based on the work of IU is

$$G(q) = A_FQ^4 + B_FQ^2 + C_F + [A_FQ^4 + D_FQ^2 - C_F]\frac{4-Q^2}{4Q}\ln\left|\frac{2+Q}{2-Q}\right| \tag{15}$$

Finally, Sarkar et. al. has presented a straightforward version of the LFCF, which is as follows

$$G(q) = A_S[1 - (1 + B_SQ^4)\exp(-C_SQ^2)] \tag{16}$$

where, $Q = 2\chi$ with $\chi = q/2k_F$

The parameters A_{VS}, B_{VS}, A_{IU}, C_{IU}, A_F, B_F, C_F, D_F, A_S, B_S, and C_S are the atomic volume-dependent parameters of VS, IU, F, and S LFCFs and are taken from ref. [28-32].

2.4. Scaling laws for transport coefficients

A straightforward link between the structural ($g(r)$) and transport properties (D and η) of liquid metals is provided by the USLs given by Rosenfeld, Dzugutov, and Li [35, 37, 38]. To determine transport coefficients, Rosenfeld took into account macroscopic reduction parameters such as temperature and density, whereas Dzugutov and Li took into account microscopic parameters such as collision frequency

and HS diameter. In liquid metals, studies of two-body, three-body, and many-body [36] consideration can approximate the thermodynamic S_{ex}. Only two-body approximations will be taken into account in this investigation. We will use the USLs of Rosenfeld et. al, Dzugutov, and Li et. al. which are described below.

Rosenfeld states that the following are the reduced diffusion coefficient D_R^* and viscosity coefficient η_R^*:

$$D_R^* = D\frac{n^{1/3}}{(kT/m)^{1/2}} \tag{17}$$

$$\eta_R^* = \eta\frac{n^{-2/3}}{(mkT)^{1/2}} \tag{18}$$

where *n* represents the number density and *T* is the temperature in kelvin. The scaling law of Dzugutov is represented as:

$$D_Z^* = 0.049e^{S_{ex}} \tag{19}$$

Li then proposed the following new relationship between S_{ex} and η_L^*:

$$\eta_L^* = 0.035e^{-0.55S_{ex}} \tag{20}$$

Where S_{ex} is given by,

$$S_{ex} = -2\pi n\int_0^\infty\{g(r)\ln[g(r)] - [g(r)-1]\}r^2dr \tag{21}$$

and approximated using the two-body *g(r).*

The USL for *D* is reformulated by Dzugutov using the microscopic parameters, collision frequency Γ, and HS diameter, *σ*. Li established a scaling relation regarding *η* following Dzugutov. Following are the reduced *D* and *η* based on the microscopic reduction parameters:

$$D_Z^* = D\frac{1}{\Gamma\sigma^2} \tag{22}$$

$$\eta_L^* = \eta\frac{\sigma}{\Gamma\mathrm{m}} \tag{23}$$

where the Enskog theory states that the collision frequency Γ is,

$$\Gamma = 4\sigma^2 g(\sigma)n(\pi kT/m)^{1/2} \tag{24}$$

where $g(\sigma)$ is the value of $g(r)$ evaluated at $r = \sigma$ (HS diameter). The position of the first principal peak of $g(r)$ usually gives an estimation of HS diameter.

3. RESULTS AND DISCUSSION

In this section, the calculated results of the temperature-dependent *D* and *η* for the liquids Mn, Pt, and Ti obtained using various screening on BS pseudopotential are presented with the qualitative argument. The calculated results are also compared with available experimental and theoretical data. It is clear from theory that the two main components of this investigation are S_{ex}, and HS diameter, *σ*. To determine

these components, $g(r)$ is needed which completely describes the structure of the liquid metals through a model potential. As a model potential, BS pseudopotential has been used with five different types of LFCF to obtain the liquid structure using the VMHNC integral theory as well as the LWCA perturbation method.

For liquid metals, the profile (*e.g*., peak position, peak height) of BS pseudopotential, $V(r)$ varies depending on the values of three essential parameters namely Z_s, a, and R_c. The parameters R_c and a should ideally be selected to provide the necessary phase shift or to provide the best match for the particular experimental result. Here, we have chosen these parameters which are obtained by fitting the experimental data [50] as closely as possible. The value of a was determined by fitting the experimental $g(r)$, as stated in [51]. The static structure factors $S(q)$ are highly dependent on variations in the parameters of R_c and a. The present investigation imposes limitations on the range of R_c/a, which is confined to the interval of $4 < R_c/a < 5$. In this interval, an evaluation of the attractive and repulsive factors that contribute to $V(r)$ holds considerable importance. The assumption of $Z_s > 1$ has been made to account for the influence of *sd* hybridization.

The number density $n(T)$ and its temperature gradient, $\frac{\partial n}{\partial T}$ are also an essential input parameter. The corresponding melting temperature is represented by T_m. The ref. [52] provides a list of $\frac{\partial n}{\partial T}$ values in units of 10^{-6} ($Å^{-3}K^{-1}$). We have taken all the other values of input parameters for liquids Ti, Mn & Pt from ref. [53]. Table 1 displays the necessary input values and Fig. 1 illustrates the profile of $V(r)$ with five different LFCFs. Fig. 1 shows that $V(r)$ of BS pseudopotential for all five LFCFs have a long oscillatory tail that runs to infinity, as also observed for liquids Ti and Pt in ref. [53]. For large values of r, these oscillations arise due to a logarithmic singularity in $G(q)$ at $q = 2k_F$. These oscillations are linked to the oscillations in the screening charge in a metal discovered by Friedel and are known as Friedel oscillations [54]. The height and the position of principle minima (i.e., well-depth) of BS potential is a crucial component. The well-depth refers to the intensity of the mutually attracting force that exists between individual atoms. The maximum height of the well is typically characterized by a minimum energy value, which represents the most stable configuration of the atoms. The depth of the BS potential changes depending on the LCFs and the system which can be seen from Panels (i), (ii), and (iii) of Fig. 1 below. As shown in this figure, the depth of the potential well owing to the LFCF of Farid et. al. is the greatest, while that due to the LFCF of Sarker et. al. is the least, in comparison to the $V(r)$ of other LFCFs whose depths fall between these two for all the concerned systems. Additionally, from Fig. 1 it can be observed that the position of the first minima in the profile of BS pseudopotential for screening of Taylor et.al. is slightly shifted to larger r while that of Farid et. al. is at the lowest r for all the concerned systems. However, the location of the first minimum as a result of the other three screening functions is between these two for all the metals considered in this study. The material in question determines the exact depth of the well, as does the quality of the fitting procedure and parameter used to produce the potential and screening function, whereas the position of the potential well's first minima is decided by the complicated interaction of all forces that attract and repel. As a result, the depth and location of the initial minimum of the model potential due to various LFCFs vary for obvious reasons [16].

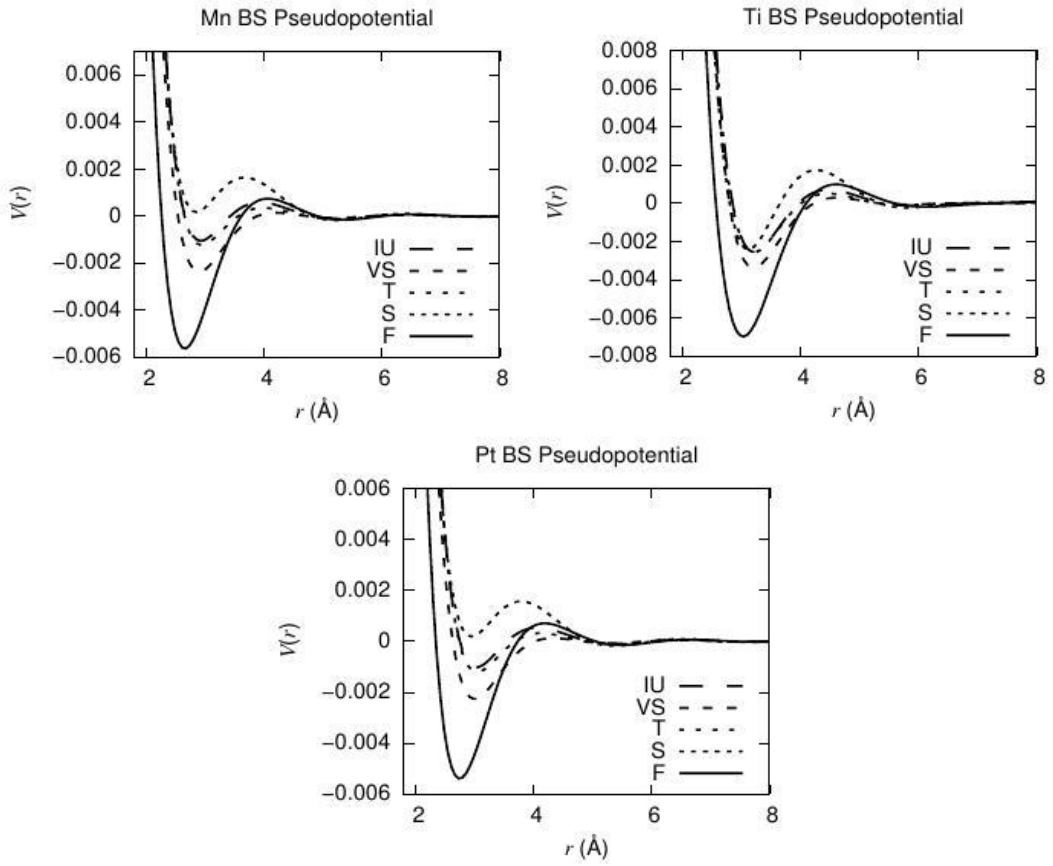

Fig. 1: Effective pair potential, *V(r)* of liquids Mn, Ti, and Pt with five different local field correction functions.

Table 1: Input parameters for the temperature-dependent number density *n*, temperature-independent core radius R_c, softness parameter *a*, effective s-electron occupancy number Z_s, number density *n* and $\frac{\partial n}{\partial T}$ are presented, at a given temperature *T*.

Systems	T**(K)**	T_m**(K)**	n**(Å^{-3})**	$\frac{\partial n}{\partial T}$	R_c **(a.u.)**	a **(a.u.)**	Z_s
Ti	1973	1958	0.0522	-8.60	1.800	0.415	1.4
Mn	1533	1514	0.0627	-7.57	1.560	0.370	1.4
Pt	2053	2042	0.0585	-8.95	1.800	0.450	1.4

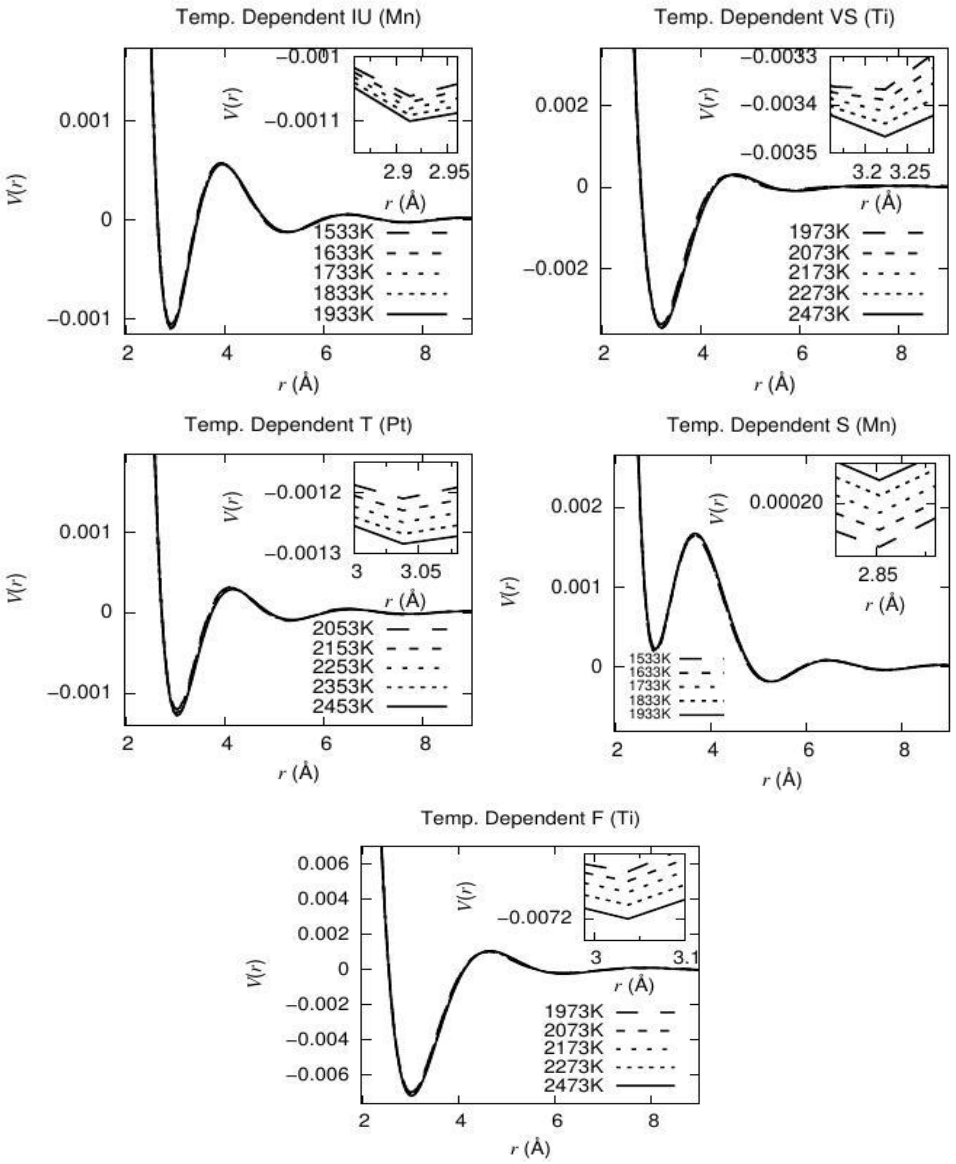

Fig. 2: Effect of temperature on potential obtained using IU, VS, T, S, and F screening functions as representatives for liquids Mn, Ti, Pt, Mn, and Ti, respectively.

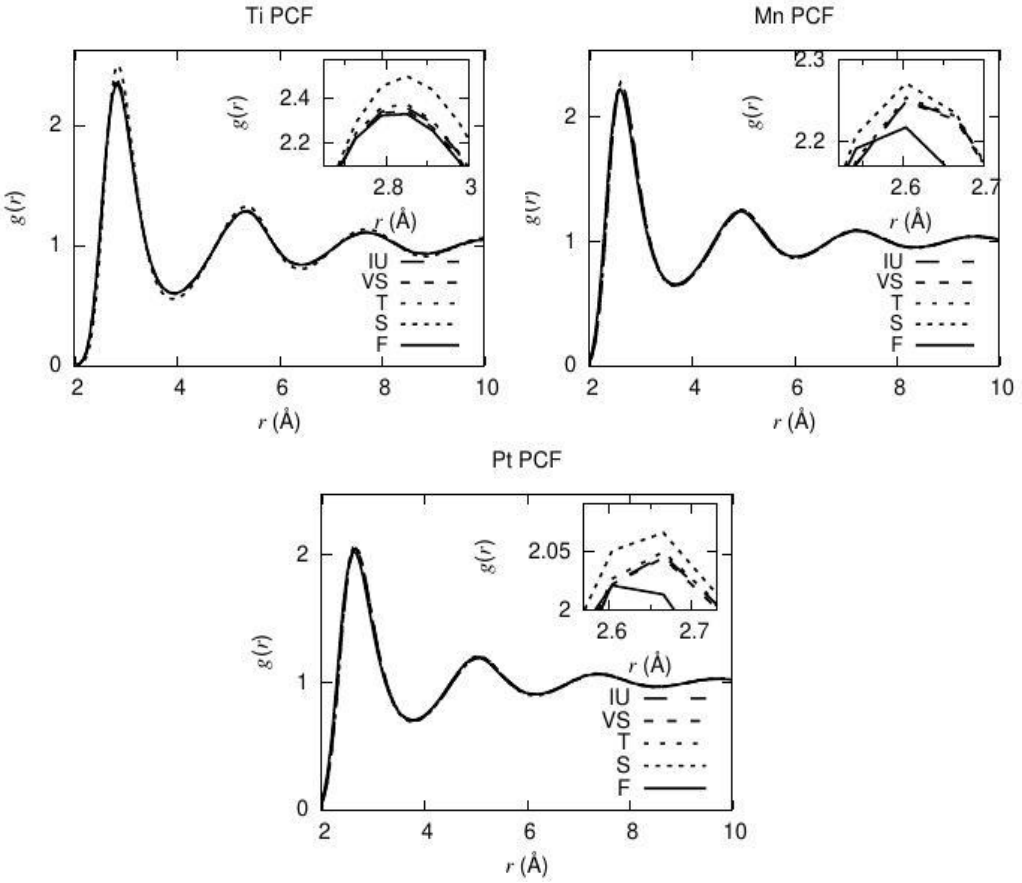

Fig. 3: Effect of screening on $g(r)$ of liquids Ti, Mn, and Pt calculated using VMHNC theory at 1973 K, 1533 K, and 2053 K, respectively.

Now, looking at the effect of temperature on the profile of $V(r)$ in Fig. 2 obtained due to concerned LFCFs it can be seen that with increasing temperature the position of first minima shifted to lower r for all the systems in the investigation. Using these effective pair potentials obtained with five different LFCFs, $g(r)$) of Mn, Pt, and Ti have been calculated at various temperatures above the melting point of the respective liquid. To determine $g(r)$, self-consistent VMHNC theory and LWCA perturbation theory are used. The complete profile of $g(r)$ is needed to calculate two-body excess entropy which is an essential ingredient to determine atomic transport properties as given by Eqn. (21). The profiles of $g(r)$ in Fig. 3 for all concerned liquids show that convergence (i.e. minimal interaction between atoms) has been achieved within the inter-atomic distance of 10 Å. The effect of different LFCFs on model potential

is visible on the profile of $g(r)$ as the peak position and peak height vary due to respective LFCFs. The position of the first principal peak of $g(r)$ which is called hard sphere diameter (HSD), σ varies slightly due to the concerned LFCFs in both VMHNC theory and LWCA method. The obtained values of the σ are almost the same while $g(r)$ was estimated using VMHNC theory combined with the potential of concerned LFCFs. On the contrary, while calculating using the LWCA method, σ was found to be at larger r for the LFCF of Taylor et. al. and at lower r for the LFCF of Farid et. al. for all the concerned liquids. The values of σ for each different LFCF with available experimental [50], simulated [55], and theoretical [56] values are listed in Table 2. The reasoning behind getting different σ values in the case of VMHNC and LWCA method although same potential has been used is as follows. σ in LWCA theory is the distance from the origin to the position where $g(r)$ begins to be non-zero and, the position lies at a little lower value of r than the principal peak position but at a higher value of r than from the position where VMHNC result begins to be non-zero. This is the main reason of discrepancy in σ between LWCA and VMHNC [57]. Furthermore, $g(\sigma)$ obtained using VMHNC theory along with BS model potential with the LFCF of Sarker et. al. is the maximum while that of Farid et. al. is the lowest. The peak heights of $g(r)$ of the remaining three LFCFs are between those of Sarker et al. and Farid et. al. for all the concerned systems. But in the case of the LWCA method, $g(\sigma)$ values for VS screening are a bit higher for Ti and Pt compared to other LFCFs. Whereas, for Mn, IU screening results in higher values of $g(\sigma)$ than other LFCFs.

Table 2: Calculated hard sphere diameter, σ for liquid transition metals obtained from VMHNC and LWCA theory combined with different BS local field correction functions are presented with available experimental (Expt.) [50], simulated (Sim.) [55], and theoretical (Theo.) [56] values.

Systems	T (K)	σ(Å)												
		VMHNC					LWCA					Expt.	Sim.	Theo.
		IU	VS	T	S	F	IU	VS	T	S	F	[50]	[55]	[56]
Mn	1533	2.606	2.606	2.604	2.606	2.604	2.544	2.544	2.604	2.482	2.421	2.60	2.57	2.55
Ti	1973	2.853	2.853	2.853	2.854	2.853	2.792	2.792	2.792	2.729	2.668	3.20	2.86	2.71
Pt	2053	2.666	2.667	2.666	2.668	2.607	2.606	2.544	2.606	2.544	2.420	2.70	-	2.63

Alongside the dependence on LFCFs, the peak height $g(\sigma)$ is also temperature-dependent. The temperature-dependent $g(\sigma)$ is a very crucial component to calculate atomic transport properties as given in Eqn. (24). At higher temperatures, particles have more kinetic energy, resulting in more thermal motion. This greater mobility disturbs the orderly arrangement of particles observed at lower temperatures. As a result, the height of the first principal peak of $g(r)$ falls as the temperature of the HS liquid rises. Temperature-dependent $g(r)$ calculated using concerned LFCFs in combination with both VMHNC and LWCA methods in Fig. 4 and Fig. 5 clearly illustrates the drop of $g(\sigma)$ with increasing temperature for all the systems under consideration. The calculated values of temperature-dependent $g(\sigma)$ using both VMHNC and LWCA methods are listed in Table 3.

Table 3: Calculated (Calc.) g(σ) at hard sphere diameter, σ for liquid transition metals obtained from VMHNC and LWCA theory combined with different BS local field correction functions are presented with available experimental (Expt.) [50] data.

Systems	*T* (K)	Calc.										Expt.
		VMHNC					LWCA					
		IU	VS	T	S	F	IU	VS	T	S	F	[50]
Mn	1533	2.214	2.236	2.239	2.253	2.207	2.731	2.614	2.704	2.476	2.155	2.333
	1633	2.181	2.167	2.187	2.195	2.149	2.559	2.579	2.641	2.420	2.063	-
	1733	2.124	2.109	2.129	2.132	2.089	2.494	2.490	2.545	2.264	1.868	-
	1833	2.073	2.063	2.075	2.079	2.043	2.437	2.368	2.397	2.282	1.948	-
	1933	2.020	2.018	2.027	2.028	2.002	2.305	2.339	2.385	2.172	1.821	-
Ti	1973	2.350	2.328	2.367	2.483	2.316	2.738	2.779	2.738	2.621	2.662	2.239
	2073	2.272	2.259	2.444	2.391	2.241	2.641	2.704	2.662	2.593	2.379	-
	2173	2.210	2.190	2.222	2.310	2.172	2.579	2.628	2.593	2.524	2.247	-
	2273	2.145	2.138	2.167	2.241	2.115	2.517	2.566	2.531	2.510	2.264	-
	2373	2.090	2.080	2.108	2.172	2.063	2.459	2.510	2.474	2.448	2.282	-
Pt	2053	2.043	2.028	2.046	2.058	2.018	2.491	2.600	2.552	2.379	2.023	-
	2153	1.198	1.994	2.001	2.008	1.970	2.402	2.552	2.431	2.218	1.937	2.573
	2253	1.954	1.945	1.958	1.963	1.931	2.448	2.207	2.310	2.247	1.880	-
	2353	1.914	1.908	1.918	1.922	1.894	2.368	2.115	2.264	2.126	1.862	-
	2453	1.874	1.876	1.879	1.880	1.859	2.121	2.103	2.287	2.052	1.779	-

Finally, using calculated values of σ, $g(\sigma)$, and S_{ex}, both diffusion and viscosity coefficients have been determined at temperatures above the corresponding melting points of the concerned liquids. It can be seen from Table 4, Table 5, and Fig. 6 that with increasing temperature D is increasing for all the concerned methods and all the metals. D rises with rising temperature because higher temperatures provide more thermal energy to particles, allowing them to overcome energy barriers more easily and diffuse quickly.

In general, regarding diffusion coefficient, the VMHNC method yields excellent results in terms of theoretical value [41] for Ti, with those obtained using the BS potential of the screening function of Taylor et. al. employing the USL of Rosenfeld et. al. exhibiting the closest alignment. On the other hand, LWCA performs well for Mn and Pt, particularly when utilizing the BS pseudopotential with the screening function of Sarker et. al applied to the scaling laws of Rosenfeld et. al. Fig. 6 depicts that calculated values while utilizing the scaling laws of Rosenfeld along with BS pseudopotential screened with LFCF of Farid et. al. in both VMHNC and LWCA method are greater than all the other calculated values for all the systems in concerned. This might be due to the lower $g(\sigma)$ values obtained both in VMHNC theory and the LWCA method while incorporating the LFCF of Farid et. al.

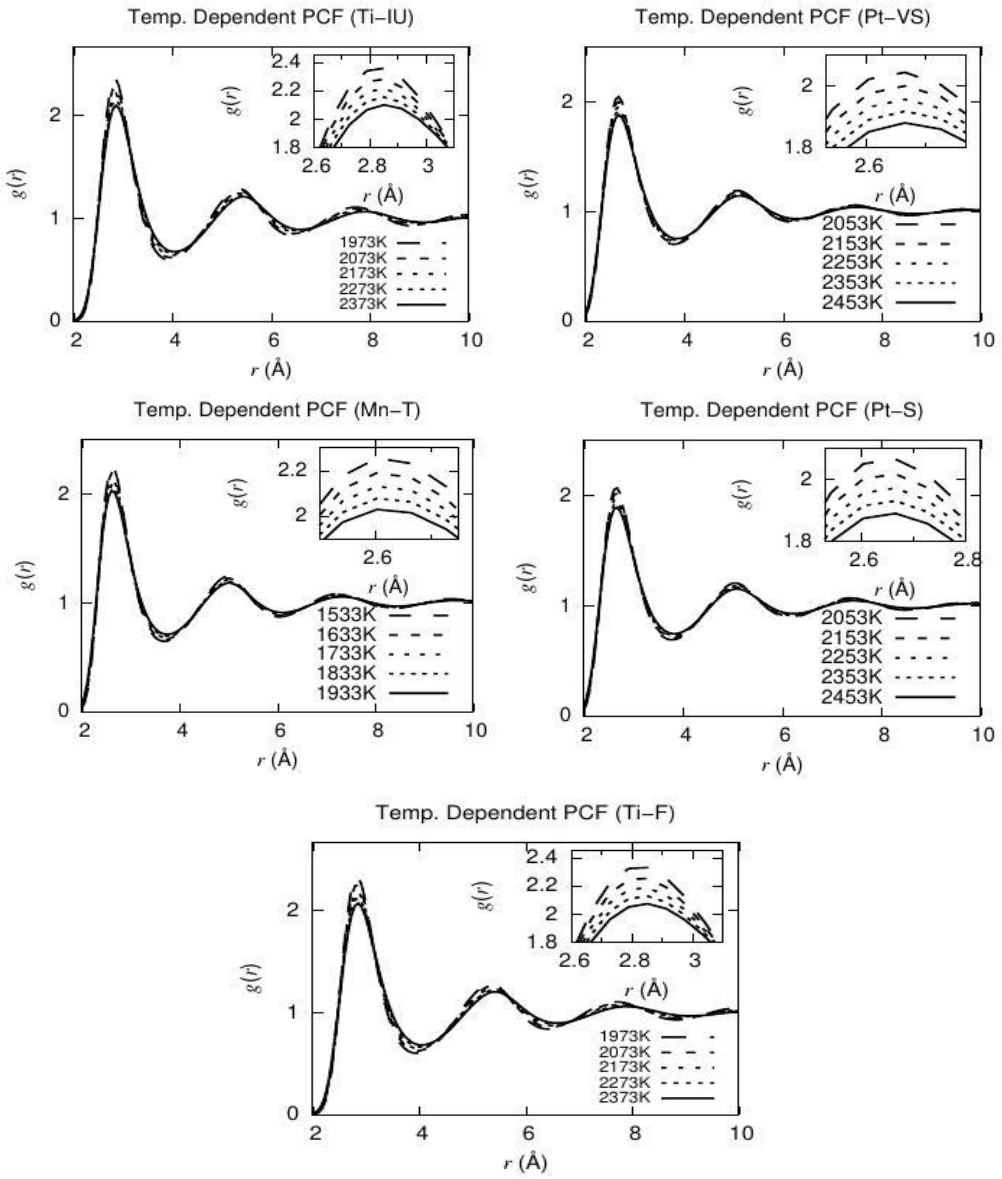

Fig. 4: Effect of temperature on *g(r)* of liquids Mn, Ti, and Pt obtained using VMHNC theory at various temperatures.

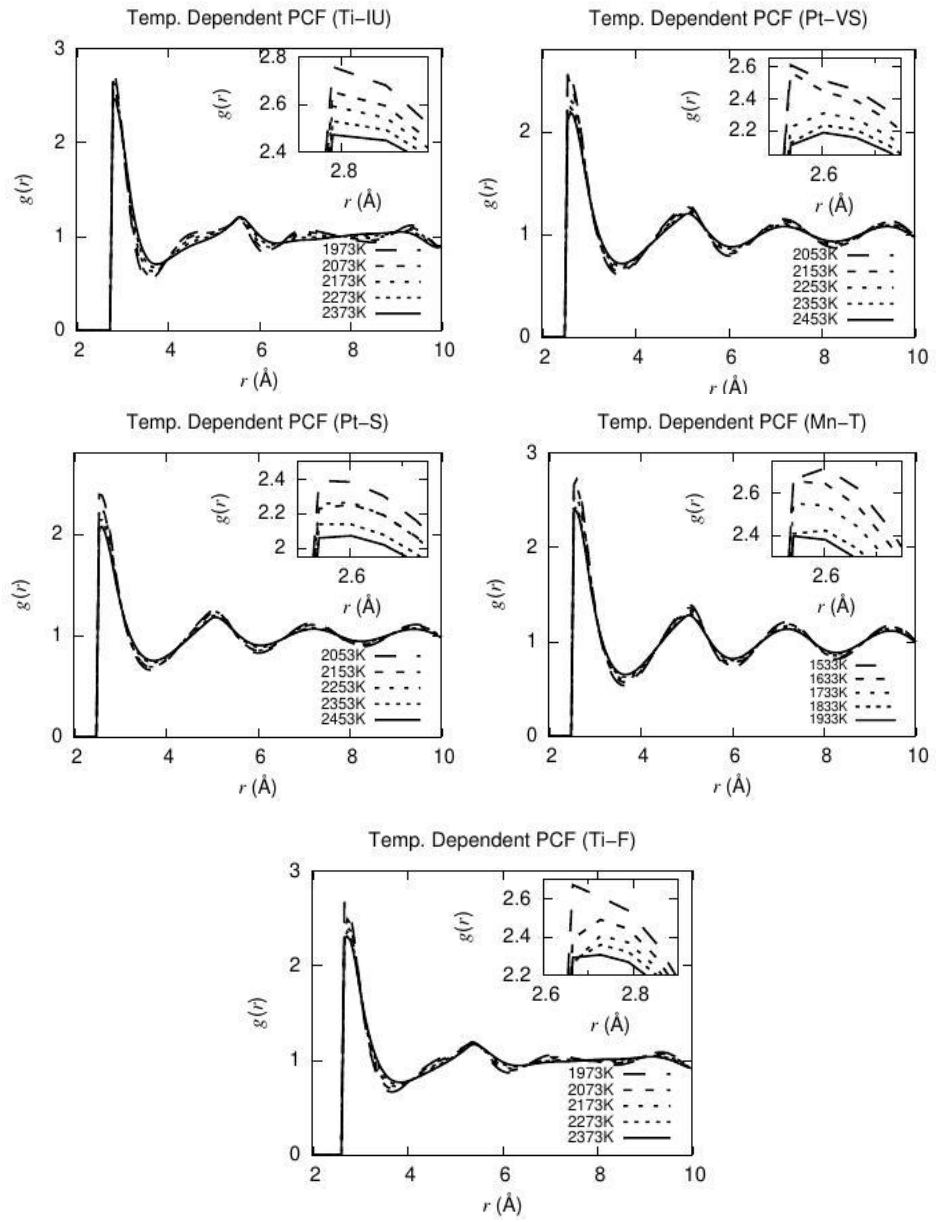

Fig. 5: Effect of temperature on $g(r)$ of liquids Mn, Ti, and Pt obtained using LWCA theory at various temperatures.

Table 4: Calculated (Calc.) diffusion coefficients, D $(10^{-9}\ m^2 s^{-1})$ for liquid transition metals obtained from Scaling laws in conjunction with VMHNC theory are compared with the available theoretical data (Theo.). *a* is taken from ref. [41] and *c*, *d* are taken from ref. [58]

Systems	T(k)	Calc.										Theo.	
		D_Z					D_R						
		IU	VS	T	S	F	IU	VS	T	S	F	[41]	[58]
Mn	1533	9.29	9.65	9.50	9.23	10.29	10.27	10.50	10.39	10.07	11.20	5.18[a]	-
	1633	11.00	11.23	11.17	10.94	12.04	12.18	12.41	12.30	12.03	13.24	-	-
	1733	12.27	12.52	12.47	12.32	13.73	13.87	14.13	14.02	13.83	15.36	-	-
	1833	13.87	14.11	14.02	13.97	15.82	15.93	16.14	16.04	15.92	17.87	-	-
	1933	15.75	15.61	15.57	15.96	17.50	18.35	18.16	18.10	18.40	20.07	-	-
Ti	1973	9.56	9.42	8.71	5.88	10.10	9.59	9.55	8.85	6.22	10.14	8.62[a]	-
	2073	11.83	12.29	11.32	8.65	12.62	11.97	12.39	11.67	8.95	12.74	-	-
	2173	14.11	13.92	13.74	10.87	14.49	14.43	14.37	14.07	11.32	14.93	-	-
	2273	15.91	16.53	15.85	12.62	16.96	16.67	17.22	16.48	13.38	17.73	-	-
	2373	18.04	18.27	17.65	14.87	19.27	19.28	19.52	18.81	16.02	20.52	-	-
Pt	2053	8.65	8.78	8.72	8.43	8.53	9.44	9.59	9.49	9.15	10.11	-	2.48[c], 2.88[d]
	2153	9.54	9.68	9.58	9.37	9.34	10.63	10.75	10.65	10.39	11.38	-	-
	2253	10.39	10.50	10.45	10.31	9.95	11.84	11.97	11.88	11.68	12.44	-	-
	2353	11.01	11.30	11.58	10.93	10.80	12.89	13.18	13.13	12.73	13.81	-	-
	2453	11.85	11.94	11.86	11.87	11.66	14.23	14.29	14.21	14.16	15.23	-	-

Next, when considering the viscosity coefficient, the overall picture reveals that both VMHNC theory and LWCA method work well for all screening functions and systems regardless of reasonable deviation of some calculated values from experimental data [52] and theoretical values in the case of the LWCA method. While the LWCA method is employed to calculate η all the LFCFs for both the scaling laws result in higher values of η except for the LFCFs of Sarker et. al. and Farid et. al. The reason behind this is the first principal values of $g(r)$ calculated using the LWCA method listed in Table 3. The data there indicate that only the $g(\sigma)$ values of Sarker et. al. and Farid et. al. are close to the experimental one. But in the case of the VMHNC method, all the calculated values of $g(\sigma)$ are consistent with the results of the experiment except for Pt. This superiority stems from VMHNC's utilization of the complete potential profile, encompassing both attractive and repulsive components, in structural calculations, whereas LWCA only incorporates the repulsive portion [8]. However, for Pt, LWCA demonstrates effectiveness, yielding values closer to theoretical ones, whereas VMHNC tends to underestimate slightly, possibly attributed to Pt's lower $g(\sigma)$ values across all screening functions and temperatures.

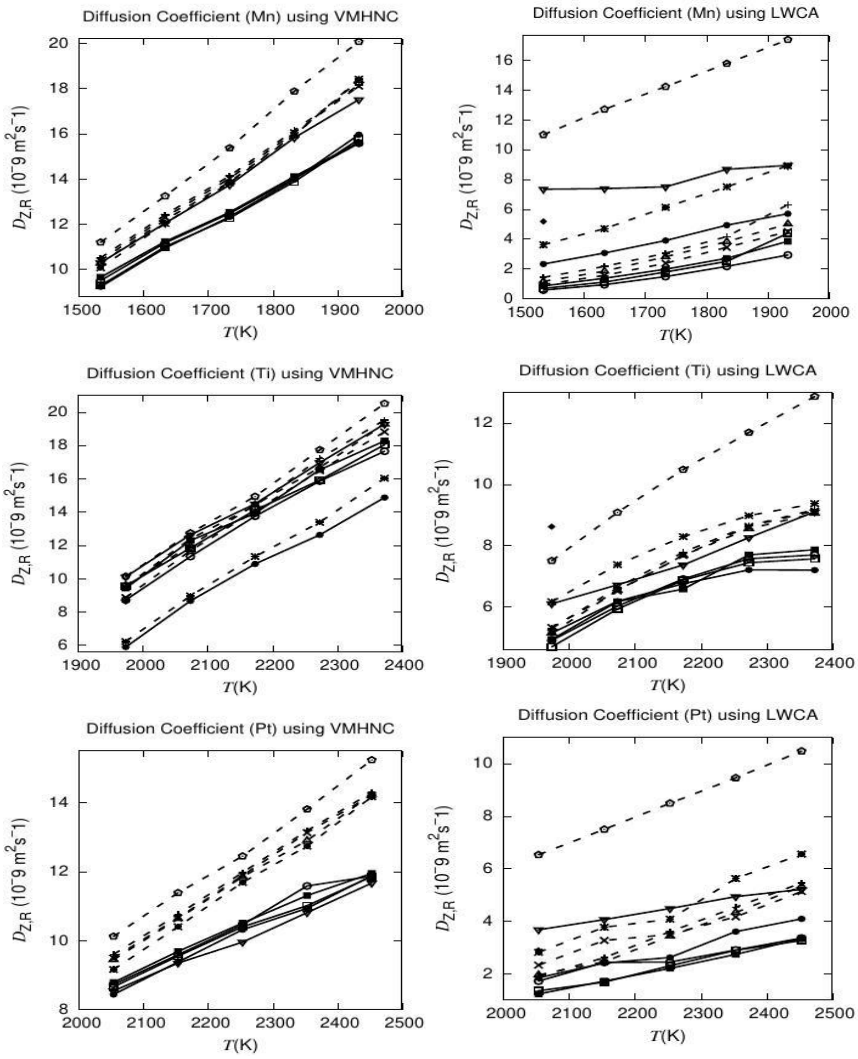

Fig. 6: Calculated temperature-dependent diffusion coefficient for liquids Mn, Ti, and Pt using five different LFCFs on BS pseudopotential along with VMHNC and LWCA method. Calculated values of *D* using scaling laws of Dzugutov are represented by solid lines with symbols empty square, filled square, empty circle, filled circle, and down triangle, respectively for LFCFs of IU, VS, T, S, and F. Again, *D* obtained using scaling laws of Rosenfeld are represented by dashed lines with symbols filled up-triangle, cross, saltire, cross & saltire, and pentagon, respectively for LFCFs of IU, VS, T, S, and F. These values are compared with available theoretical data [41, 58] presented by symbols diamond.

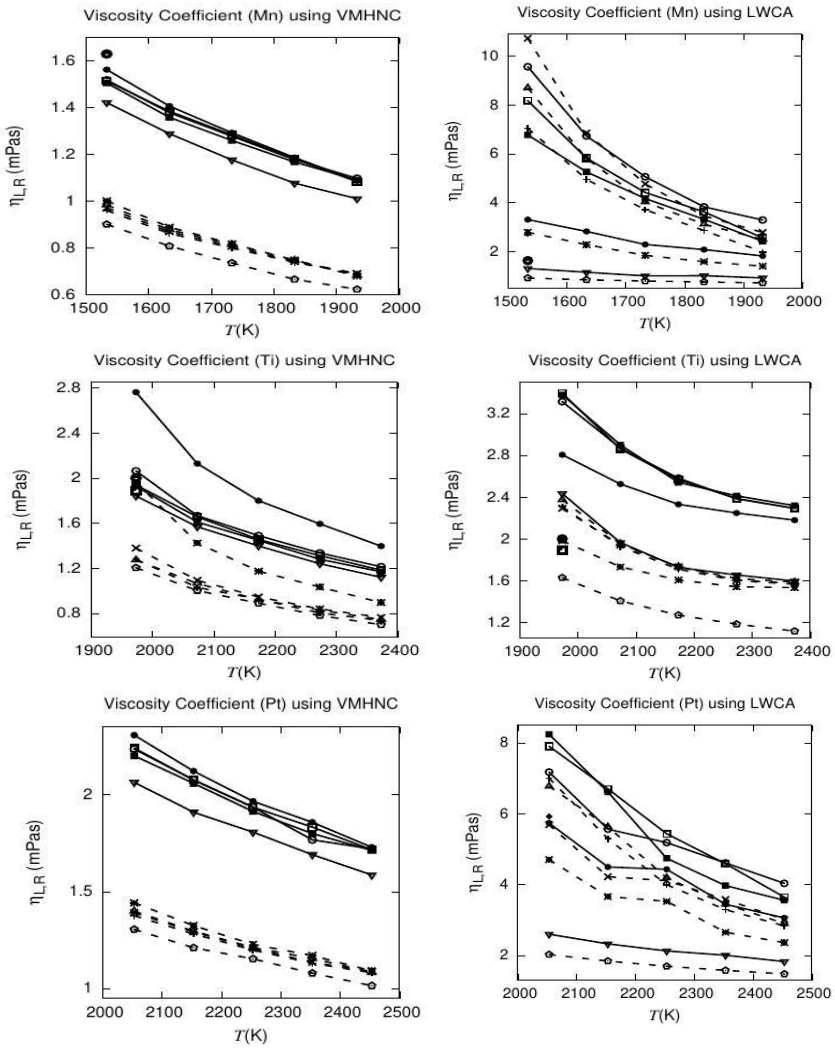

Fig. 7: Calculated temperature-dependent viscosity coefficient for liquids Mn, Ti, and Pt using five different LFCFs on BS pseudopotential along with VMHNC and LWCA method. Calculated values of η using scaling laws of Li are represented by solid lines with symbols empty square, filled square, empty circle, filled circle, and down triangle, respectively for LFCFs of IU, VS, T, S, and F. Again, η obtained using scaling laws of Rosenfeld are represented by dashed lines with symbols filled up-triangle, cross, saltire, cross & saltire, and pentagon, respectively for LFCFs of IU, VS, T, S, and F. These values are compared with available experimental data [52] presented by symbols square with a white dot and theoretical data [41, 58] presented by symbols diamond & filled circle with a white dot.

Table 5: Calculated (Calc.) diffusion coefficients, D ($10^{-9}\ m^2 s^{-1}$) for liquid transition metals obtained from Scaling laws in conjunction with LWCA theory are compared with the available theoretical data (Theo.). *a* is taken from ref. [41] and *c*, *d* are taken from ref. [58]

Systems	T(k)	Calc.										Theo.	
		D_Z					D_R						
		IU	VS	T	S	F	IU	VS	T	S	F	[41]	[58]
Mn	1533	0.68	0.85	0.57	2.31	7.34	1.16	1.43	0.94	3.61	10.99	5.18[a]	-
	1633	1.11	1.36	0.93	3.05	7.38	1.84	2.16	1.56	4.69	12.70	-	-
	1733	1.78	1.97	1.47	3.89	7.50	2.80	3.04	2.37	6.12	14.22	-	-
	1833	2.49	2.70	2.15	4.92	8.67	3.81	4.16	3.44	7.50	15.77	-	-
	1933	4.38	3.84	2.92	5.69	8.94	5.00	6.30	4.49	8.92	17.37	-	-
Ti	1973	4.69	4.93	4.90	5.14	6.10	5.14	5.29	5.32	6.16	7.50	8.62[a]	-
	2073	5.92	6.17	6.02	6.18	6.72	6.53	6.62	6.51	7.37	9.08	-	-
	2173	6.87	6.57	6.90	6.75	7.36	7.68	7.78	7.68	8.29	10.48	-	-
	2273	7.44	7.70	7.57	7.20	8.26	8.55	8.65	8.63	8.98	11.69	-	-
	2373	7.57	7.86	7.69	7.20	9.10	9.05	9.17	9.13	9.37	12.85	-	-
Pt	2053	1.34	1.22	1.70	1.83	3.67	1.94	1.88	2.32	2.80	6.53	-	2.48[c], 2.88[d]
	2153	1.67	1.71	2.42	2.40	4.05	2.44	2.60	3.26	3.76	7.49	-	-
	2253	2.29	2.19	2.43	2.61	4.47	3.42	3.59	3.49	4.07	8.49	-	-
	2353	2.88	2.73	2.89	3.59	4.93	4.32	4.52	4.16	5.62	9.46	-	-
	2453	3.25	3.33	3.35	4.08	5.20	5.32	5.45	5.12	6.55	10.48	-	-

The difference in the obtained results for D and η utilizing both VMHNC and LWCA methods for Ti, Mn, and Pt might be attributed to the varying nature of interatomic interactions in these metals. Both VMHNC and LWCA theory have been derived from the different theoretical grounds. Liquid structure of Ti is usually complex than those of liquids Mn and Pt. Therefore, exact reason behind the difference in the obtained results for D and η is still unknown to us and needs a systematic study which will remain as our future work.

Table 6: Calculated (Calc.) shear viscosity coefficients, η (*mPas*) for liquid transition metals obtained from Scaling laws in conjunction with VMHNC theory are compared with the available experimental (Expt.) [52] and Theoretical data (Theo.) [41, 57]. *a*, *b* are taken from ref. [41] and *c*, *d* are taken from ref. [58]

Systems	T (K)	Calc.										Expt.	Theo.	
		η_L					η_R							
		IU	VS	T	S	F	IU	VS	T	S	F	[52]	[41]	[58]
Mn	1533	1.51	1.50	1.51	1.56	1.42	0.98	0.96	0.97	1.00	0.90	-	$2.73^a, 1.63^b$	-
	1633	1.38	1.35	1.37	1.40	1.28	0.87	0.86	0.87	0.88	0.80	-		-
	1733	1.28	1.26	1.27	1.29	1.17	0.81	0.80	0.80	0.81	0.73	-		-
	1833	1.18	1.16	1.17	1.18	1.07	0.74	0.73	0.74	0.74	0.66	-		-
	1933	1.08	1.09	1.09	1.08	1.01	0.68	0.68	0.69	0.68	0.62	-		-
Ti	1973	1.93	1.92	2.06	2.76	1.84	1.27	1.28	1.37	1.96	1.20	5.20	$2.00^a, 1.89^b$	-
	2073	1.65	1.61	1.66	2.12	1.56	1.06	1.03	1.09	1.42	1.00	-	-	-
	2173	1.45	1.44	1.49	1.79	1.39	0.92	0.92	0.94	1.17	0.89	-	-	-
	2273	1.31	1.28	1.33	1.59	1.24	0.83	0.80	0.84	1.03	0.78	-	-	-
	2373	1.18	1.16	1.21	1.39	1.12	0.74	0.73	0.76	0.89	0.70	-	-	-
Pt	2053	2.24	2.20	2.23	2.30	2.06	1.39	1.37	1.39	1.44	1.30	-	-	$6.24^c, 5.92^d$
	2153	2.07	2.05	2.07	2.12	1.91	1.29	1.28	1.29	1.32	1.21	-	-	-
	2253	1.93	1.91	1.93	1.96	1.80	1.21	1.19	1.20	1.22	1.15	-	-	-
	2353	1.83	1.80	1.76	1.85	1.69	1.15	1.13	1.13	1.17	1.07	-	-	-
	2453	1.71	1.71	1.72	1.72	1.58	1.08	1.08	1.08	1.09	1.01	-	-	-

Table 7: Calculated (Calc.) shear viscosity coefficients, η (*mPas*) for liquid transition metals obtained from Scaling laws in conjunction with LWCA theory are compared with the available experimental (Expt.) [52] and Theoretical data (Theo.) [41, 57]. *a*, *b* are taken from ref. [41] and *c*, *d* are taken from ref. [58]

Systems	T (K)	Calc.										Expt.	Theo.	
		η_L					η_R							
		IU	VS	T	S	F	IU	VS	T	S	F	[52]	[41]	[58]
Mn	1533	8.17	6.77	9.56	3.30	1.30	8.70	7.04	10.72	2.79	0.91	-	$2.73^a, 1.63^b$	-
	1633	5.82	5.26	6.73	2.82	1.15	5.81	4.95	6.85	2.28	0.84	-		-
	1733	4.42	4.17	5.06	2.28	1.00	4.02	3.71	4.76	1.84	0.79	-		-
	1833	3.62	3.32	3.83	2.08	1.01	3.12	2.86	3.46	1.58	0.75	-		-
	1933	2.55	2.42	3.29	1.82	0.91	2.49	1.98	2.78	1.40	0.72	-		-
Ti	1973	3.39	3.38	3.31	2.80	2.43	2.37	2.30	2.29	1.98	1.62	5.20	$2.00^a, 1.89^b$	-
	2073	2.86	2.90	2.87	2.52	1.96	1.95	1.92	1.94	1.73	1.40	-	-	-
	2173	2.56	2.54	2.58	2.33	1.72	1.73	1.70	1.73	1.60	1.26	-	-	-
	2273	2.38	2.41	2.38	2.24	1.65	1.61	1.60	1.60	1.54	1.18	-	-	-
	2373	2.29	2.31	2.29	2.17	1.59	1.58	1.56	1.57	1.53	1.11	-	-	-
Pt	2053	7.90	8.24	7.17	5.73	2.59	6.77	7.00	5.69	4.70	2.02	-	-	$6.24^c, 5$
	2153	6.70	6.61	5.56	4.49	2.32	5.63	5.29	4.22	3.66	1.83	-	-	-
	2253	5.43	4.74	5.18	4.43	2.12	4.18	3.99	4.10	3.52	1.68	-	-	-
	2353	4.58	3.97	4.61	3.44	2.00	3.44	3.29	3.57	2.65	1.57	-	-	-
	2453	3.64	3.55	4.03	3.05	1.82	2.90	2.83	3.01	2.35	1.47	-	-	-

4. CONCLUSIONS

The diffusion coefficient and viscosity coefficient for liquid transition metals namely, Ti, Mn, and Pt have been studied using the USLs derived by Rosenfeld, Dzugutov, and Li in conjunction with VMHNC and LWCA methods which provide $g(r)$. We investigated the impact of various screening functions on BS pseudopotential in order to find an appropriate $g(r)$ that appropriately describes our systems. This study concludes that D increases and η decreases with increasing temperature which are consistent with available literatures. The combination of Rosenfeld's scaling laws and Farid et al.'s BS pseudopotential screening in both VMHNC and LWCA methods, provides higher calculated values of D for all concern systems. Obtained smaller $g(\sigma)$ values in the case of both VMHNC and LWCA theories are the possible reason behind this. However, the VMHNC approach provides reliable diffusion coefficient results for Ti, along with the BS pseudopotential with LFCF of Taylor et. al. and Rosenfeld scaling law. On the other hand, LWCA excels for Mn and Pt, while particularly using the BS pseudopotential with screening function Sarker et. al. and scaling laws Rosenfeld et. al. Again, in the case of η, the LWCA method generally yields higher values except for the LFCFs of Sarker et al. and Farid et al., whose $g(\sigma)$ values align closely with experimental data. In contrast, the VMHNC method consistently produces accurate $g(\sigma)$ values, except for Pt.

ACKNOWLEDGEMENTS

The Bose Centre for Advanced Study and Research in Natural Sciences, University of Dhaka, is greatly acknowledged for providing a fellowship to Md. Shakil Khan for conducting this research work.

REFERENCES

[1] S. D. Korkmaz and Ş. Korkmaz. "Investigation of atomic transport and surface properties of liquid transition metals using scaling laws." Journal of Molecular Liquids 150 (2009) 81-85. https://doi.org/10.1016/j.molliq.2009.10.005

[2] R. C. Gosh, I. M. Syed, Z. Amin and G. M. Bhuiyan. "A comparative study on temperature dependent diffusion coefficient of liquid Fe." Physica B: Condensed Matter 426 (2013) 127-131. https://doi.org/10.1016/j.physb.2013.06.022

[3] S. D. Korkmaz, and Ş. Korkmaz. "Atomic transport properties of liquid alkaline earth metals: a comparison of scaling laws proposed for diffusion and viscosity." Modelling and Simulation in Materials Science and Engineering 15 (2007) 285. https://doi.org/10.1088/0965-0393/15/3/007

[4] Y. A. Sonvane, P. B. Thakor, and A. R. Jani. "Atomic transport and surface properties of some simple liquid metal using one component plasma system." Journal of Theoretical and Applied Physics 6 (2012) 1-6. https://doi.org/10.1186/2251-7235-6-43

[5] P. B. Thakor, Y. A. Sonvane, and A. R. Jani. "Theoretical Investigation of atomic transport properties of 4d transition metals in liquid phase." Advanced Materials Research 665 (2013) 136-142. https://doi.org/10.4028/www.scientific.net/AMR.665.136

[6] H. M. Lu, G. Li, Y. F. Zhu and Q. Jiang. "Temperature dependence of self-diffusion coefficient in several liquid metals." Journal of Non-crystalline solids 352 (2006) 2797-2800. https://doi.org/10.1016/j.jnoncrysol.2006.03.049

[7] R. C. Gosh, S. B. Noor and M. A. M. Islam. "A comparative study on atomic transport properties of liquid less-simple metals." Modelling and Simulation in Materials Science and Engineering 29 (2020) 025003. https://doi.org/10.1088/1361-651X/abce43.
[8] M. S. Uddin, R. C. Gosh and G. M. Bhuiyan. "Investigation of surface tension, viscosity and diffusion coefficients for liquid simple metals. " Journal of Non-Crystalline Solids 499 (2018) 426-433. https://doi.org/10.1016/j.jnoncrysol.2018.07.014

[9] F. Zahid, G. M. Bhuiyan, S. Sultana, M. A. Khaleque, R. I. M. A. Rashid, and S. M. M. Rahman. "Investigations of the static and dynamic properties of liquid less simple metals. " physica status solidi (b) 215 (1999) 987-998. https://doi.org/10.1002/(SICI)1521-3951(199910)215:2<987::AID-PSSB987>3.0.CO;2-E
[10] F. Zahid, G. M. Bhuiyan, M. A. Khaleque, and R. I. M. A. Rashid. "Calculations of structure and shear viscosity for less simple liquid metals. " Journal of non-crystalline solids 250 (1999) 107-110. https://doi.org/10.1016/S0022-3093(99)00220-3
[11] M. A. Khaleque, G. M. Bhuiyan, and R. I. M. A. Rashid. Internal report, The Abdus salam international centre for theoretical physics. Vol. 11. IC/98/6, 1998.
[12] W. A. Harrison. "Transition-metal pseudopotentials." Physical Review 181 (1969) 1036. https://doi.org/10.1103/PhysRev.181.1036
[13] J. M. Wills, and W. A. Harrison. "Interionic interactions in transition metals." Physical Review B 28 (1983) 4363. https://doi.org/10.1103/PhysRevB.28.4363.
[14] J. T. M. D. Hosson, Atomic Configurations and Electronic Structures of Edge Dislocations (The Netherlands: Rijksuniversiteit Groningen, 1976).
[15] B. A. Oli, Nuovo Cim. 10 (1966) 48.
[16] J. L. Bretonnet, and M. Silbert. "Interionic interactions in transition metals. Application to vanadium." Physics and Chemistry of Liquids 24 (1992) 169-176. https://doi.org/10.1080/00319109208027266
[17] N. W. Ashcroft, "Electron-ion pseudopotentials in metals." Physics Letters 23 (1966) 48-50. https://doi.org/10.1016/0031-9163(66)90251-4
[18] T. C. Lim. "Connection among classical interatomic potential functions." Journal of mathematical chemistry 36 (2004) 261-269. https://doi.org/10.1023/B:JOMC.0000044223.40611.00
[19] M. W. Finnis and J. E. Sinclair. "A simple empirical N-body potential for transition metals." Philosophical Magazine A 50 (1984) 45-55. https://doi.org/10.1080/01418618408244210.
[20] M. S. Daw and M. I. Baskes. "Embedded-atom method: Derivation and application to impurities, surfaces, and other defects in metals." Physical Review B 29 (1984) 6443. https://doi.org/10.1103/physrevb.29.6443.
[21] R. Kumar and J. Singh. "Tersoff and REBO Potentials." In Forcefields for Atomistic-Scale Simulations: Materials and Applications 187-203. (Singapore: Springer Nature Singapore, 2022). https://doi.org/10.1007/978- 981-19-3092-8_9
[22] M. A. M. Islam, R. C. Gosh and G. M. Bhuiyan. "Calculation of electrical resistivity of Na-based liquid binary alkali alloys." Journal of Molecular Liquids 290 (2019) 111224. https://doi.org/10.1016/j.molliq.2019.111224
[23] S. Sharmin, G. M. Bhuiyan, M. A. Khaleque, R. I. M. A. Rashid and S. M. Mujibur Rahman. "Electronic Transport Properties of Liquid Less-Simple Metals." physica status solidi (b) 232 (2002) 243-253. https://doi.org/10.1002/1521-3951(200208)232:2<243::AID-PSSB243>3.0.CO;2-W
[24] R. C. Gosh, M. R. Amin and G. M. Bhuiyan. "Atomic transport for liquid noble and transition metals using scaling laws." Journal of Molecular Liquids 188 (2013) 148-154. https://doi.org/10.1016/j.molliq.2013.09.034
[25] R. C. Gosh, A. Z. Z. Ahmed and G. M. Bhuiyan. "Investigation of surface entropy for liquid less simple metals." The European Physical Journal B 56 (2007) 177-181. https://doi.org/10.1140/epjb/e2007-00104-9

[26] M. A. M. Islam, R. C. Gosh, F. I. Abbas and G. M. Bhuiyan. "Effects of interionic pair interactions on atomic transport properties of liquid Al." Indian Journal of Physics (2021) 1-10. https://doi.org/10.1007/s12648-021-02019-y
[27] A. M. Vora. "Electrical transport properties of liquid alloys." Physics and Chemistry of Liquids 46 (2008) 213-222. https://doi.org/10.1080/00319100701548434
[28] P. Vashishta and K. S. Singwi. "Electron correlations at metallic densities. V." Physical Review B 6, no. 3 (1972): 875. https://doi.org/10.1103/PhysRevB.6.875
[29] R. Taylor. "A simple, useful analytical form of the static electron gas dielectric function." Journal of Physics F: Metal Physics 8 (1978) 169. https://doi.org/10.1088/0305-4608/8/8/011
[30] S. Ichimaru and K. Utsumi. "Analytic expression for the dielectric screening function of strongly coupled electron liquids at metallic and lower densities." Physical Review B 24 (1981) 7385. https://doi.org/10.1103/PhysRevB.24.7385
[31] B. Farid, V. Heine, G. E. Engel and I. J. Robertson. "Extremal properties of the Harris-Foulkes functional and an improved screening calculation for the electron gas." Physical Review B 48 (1993) 11602. https://doi.org/10.1103/PhysRevB.48.11602
[32] A. Sarkar, D. Sen, S. Haldar and D. Roy. "Static local field factor for dielectric screening function of electron gas at metallic and lower densities." Modern Physics Letters B 12 (1998) 639-648. https://doi.org/10.1142/S0217984998000755
[33] S. M. M. Rahman and L. B. Bhuiyan. "Temperature dependence of atomic transport in less-simple liquid metals." Physical Review B 33 (1986) 7243. https://doi.org/10.1103/PhysRevB.33.7243
[34] M. Manna and R. C. Gosh. "Calculation of diffusion coefficient of liquid less simple metals." Physica B: Condensed Matter 649 (2023) 414482. https://doi.org/10.1016/j.physb.2022.414482
[35] M. Dzugutov. "addendum: A universal scaling law for atomic diffusion in condensed matter." Nature 411 (2001) 720-720. https://doi.org/10.1038/35079655
[36] I. Yokoyama and S. Tsuchiya. "Excess entropy, diffusion coefficient, viscosity coefficient and surface tension of liquid simple metals from diffraction data." Materials Transactions 43 (2002) 67-72. https://doi.org/10.2320/matertrans.43.67
[37] G. X. Li, C. S. Liu and Z. G. Zhu. "Excess entropy scaling for transport coefficients: diffusion and viscosity in liquid metals." Journal of non-crystalline solids 351 (2005) 946-950. https://doi.org/10.1016/j.jnoncrysol.2005.02.006
[38] Y. Rosenfeld. "A quasi-universal scaling law for atomic transport in simple fluids." Journal of Physics: Condensed Matter 11 (1999) 5415. https://doi.org/10.1088/0953-8984/11/28/303
[39] S. Yang, S. Xuping, J. Wang, F. Yin, Z. Li, S. Chen and C. Liu. "Temperature-evolution of structure and diffusion properties of liquid transition metals." Journal of non-crystalline solids 356 (2010) 1061-1069. https://doi.org/10.1016/j.jnoncrysol.2010.01.013
[40] J. L. Bretonnet. "Self-diffusion coefficient of dense fluids from the pair correlation function." The Journal of chemical physics 117 (2002) 9370-9373. https://doi.org/10.1063/1.1516594
[41] P. B. Thakor, Y. A. Sonvane and A. R. Jani. "Atomic transport properties of 3d liquid transition metals." In AIP Conference Proceedings, American Institute of Physics 1447 (2012) 915-916. https://doi.org/10.1063/1.4710300
[42] J. K. Percus and G. J. Yevick. "Analysis of classical statistical mechanics by means of collective coordinates." Physical Review 110 (1958) 1. https://doi.org/10.1103/PhysRev.110.1
[43] Y. Rosenfeld. "Comments on the variational modified-hypernetted-chain theory for simple fluids." Journal of statistical physics 42 (1986) 437-457. https://doi.org/10.1007/BF01127720
[44] A. Meyer, M. Silbert and W. H. Young. "A simplified WCA theory of liquid structure." Chemical Physics 49 (1980) 147-152. https://doi.org/10.1016/0301-0104(80)85048-8

[45] G. M. Bhuiyan, J. L. Bretonnet and M. Silbert. "Liquid structure of the 3d transition metals." Journal of non-crystalline solids 156 (1993) 145-148. https://doi.org/10.1016/0022-3093(93)90149-R
[46] N. Jakse and J. L. Bretonnet. "Structure and thermodynamics of liquid transition metals: integral-equation study of Fe, Co and Ni." Journal of Physics: Condensed Matter 7 (1995) 3803. https://doi.org/10.1088/0953-8984/7/20/002
[47] L. E. González, A. Meyer, M. P. Iniguez, D. J. González and M. Silbert. "Liquid structure of the alkaline-earth metals." Physical Review E 47 (1993) 4120. https://doi.org/10.1103/PhysRevE.47.4120
[48] J. D. Weeks, D. Chandler and H. C. Andersen. "Role of repulsive forces in determining the equilibrium structure of simple liquids." The Journal of chemical physics 54 (1971) 5237-5247. https://doi.org/10.1063/1.1674820
[49] P. Swan. "Deduction of non-singular potentials from scattering phase shifts (II). Charged particles." Nuclear Physics A 90 (1967) 436-448. https://doi.org/10.1016/0375-9474(67)90246-1
[50] Y. Waseda. "The structure of non-crystalline materials." Liguids and Amorphous Solids (1980). https://doi.org/10.1016/0025-5416(82)90073-8.
[51] G. M. Bhuiyan, M. Silbert and M. J. Stott. "Structure and thermodynamic properties of liquid transition metals: An embedded-atom-method approach." Physical Review B 53 (1996) 636. https://doi.org/10.1103/PhysRevB.53.636
[52] J. C. Smithells, Metals Reference Book, 5th edition (London: Butterworths, 1976).
[53] R. C. Gosh, R. Das, S. C. Sen and G. M. Bhuiyan. "Surface entropy of liquid transition and noble metals." Surface Science 637 (2015) 63-68. https://doi.org/10.1016/j.susc.2015.03.014
[54] O. P. Sharma. "A pseudopotential study of the electronic properties of noble metals." Physica Status Solidi B Basic Research 86 (1978) 483-492. https://doi.org/10.1002/pssb.2220860206
[55] N. Jakse, J. F. Wax, J. L. Bretonnet and A. Pasturel. "Structure and thermodynamics of the 3d-transition metals in the liquid state." Journal of non-crystalline solids 205 (1996) 434-437. https://doi.org/10.1016/S0022-3093(96)00255-4
[56] P. B. Thakor, Y. A. Sonvane and A. R. Jani. "Structural properties of some liquid transition metals." Physics and Chemistry of Liquids 49 (2011) 530-549. https://doi.org/10.1080/00319104.2010.508040
[57] R.C. Gosh, M.R. Amin, A.Z. Ziauddin Ahmed, I. M. Syed, G.M. Bhuiyan, Calculation of surface entropy of liquid transition and noble metals, Applied Surface Science 258 (2012) 5527–5532. https://doi.org/10.1016/j.apsusc.2011.11.118
[58] M. M. G. Alemany, L. J. Gallego, L. E. González and D. J. González. "A molecular dynamics study of the transport coefficients of liquid transition and noble metals using effective pair potentials obtained from the embedded atom model." The Journal of Chemical Physics 113 (2000) 10410-10411. https://doi.org/10.1063/1.1322626